VOLUME 35(1992), 4, 724–730
TRIBOLOGY TRANSACTIONS

Visco-Elastic Effects in MIL-L-7808-Type Lubricant Part III: Model Implementation in Bearing Dynamics Computer Code©

P. K. GUPTA (Member, STLE)
PKG Inc.
Clifton Park, New York 12065

Modeling of the dynamic performance of a high-speed ball bearing is carried out as a function of the visco-elastic behavior of the lubricant. For a given bearing geometry and a set of operating conditions, the cage motion becomes relatively unstable as the lubricant shear modulus and critical shear stress values are varied to introduce increased elastic effects and lower traction coefficients. A potential for correlation of bearing instabilities to fundamental properties of the lubricant is thereby demonstrated.

KEY WORDS

Rolling Bearing Dynamics, EHD, Lubricant Traction

INTRODUCTION

The dynamic performance of rolling bearings has been known to be greatly influenced by the traction behavior of the lubricant. Very often, the instabilities in the motion of the bearing elements are attributed to the rheological behavior of the lubricant in the rolling/sliding contacts between the rolling elements and the interacting races. Modeling the traction behavior of a lubricant in a concentrated contact has, therefore, been a problem of significant interest over the past many years. This paper is the third part of an investigation aimed at modeling the behavior of the MIL-L-7808-type lubricant. Analytical formulation of the traction model is the subject of the first part (*1*), model correlation to experimental traction data and the development of the various rheological constants is undertaken in the second part (*2*), and finally, the implementation of the model in a bearing dynamics computer code is considered in the present paper.

Correlation of bearing performance to the level of internal friction in the bearing has been modeled by a number of investigators, (*3*)–(*5*). Similarly, a rather vast amount of the available literature has been devoted to relating the friction or traction behavior to the fundamental properties of the lubricant. Thus, by combining the bearing dynamics and lubricant traction model it may be possible to correlate the overall bearing performance to the fundamental constitutive behavior of the lubricant. A demonstration of such a feasibility is the primary objective of the present investigation. The traction models, based on the work of Johnson and Tevaarwerk (*6*), and Bair and Winer (*7*), are incorporated into an available bearing dynamics computer code ADORE (*8*). Dynamic performance simulations of a bearing are then undertaken to show a direct relation between fundamental lubricant properties and bearing instabilities.

**Presented at the 46th Annual Meeting
in Montreal, Quebec, Canada
April 29–May 2, 1991
Final manuscript approved July 17, 1991**

NOMENCLATURE

- a = semi-major axis of the Hertzian contact ellipse, m
- b = semi-minor axis of the Hertzian contact ellipse, m
- D = Deborah number
- G = lubricant shear modulus, Pa
- h = lubricant film thickness, m
- H = hardness of the cage material, Pa
- K = Archard wear coefficient
- P = contact load, N
- $\bar{s}$ = dimensionless strain rate
- t = time, S
- T = time, S
- u_x = slip velocity in the x direction, M/S
- u_y = slip velocity in the y direction, M/S
- U = rolling velocity, m/s
- V = sliding velocity, m/s
- W = time-averaged wear rate M^3/S
- x,y = coordinates in the Hertzian contact ellipse
- x,y,z = bearing coordinate frame
- μ = viscosity, Pa.S
- τ_x = shear stress in the x-direction, Pa
- τ_y = shear stress in the y-direction, Pa
- τ_e = effective shear stress, Pa

MODELING APPROACH

There are two parts to modeling the traction behavior of a lubricant, the calculation of the lubricant film thickness, and the computation of traction in the concentrated contact. Implementation of film thickness equations as presented in (*1*), based on the work by Hamrock and Dowson (*9*), and Wilson and Sheu (*10*), is quite straightforward. The various equations are simply coded into relevant computational modules and then incorporated in the bearing dynamics code ADORE (*8*). Incorporation of the traction models, however, requires some further generalization before the models developed for unidirectional sliding can be implemented into a more complex ball/race contact, where the relative slip vector can vary fairly arbitrarily with respect to the rolling velocity vector. The formulation presented below is based on the work by Johnson and Tevaarwerk (*6*). In fact, the modeling procedure is also very similar to that considered by McCool (*11*) in a very recent investigation.

As proposed by Johnson and Tevaarwerk (*6*), generalization of the fundamental shear stress and strain rate equation to permit slip in both the rolling and transverse directions is accomplished by introducing an equivalent shear stress, τ_e, which basically defines an effective yield stress according to the classical von-Mises yield criteria

$$\tau_e = [\tau_x^2 + \tau_y^2]^{1/2} \qquad [1]$$

where τ_x and τ_y are shear stresses in the x and y directions, shown schematically in Fig. 1.

In terms of the above equivalent stress, the traction equation is generalized as:

$$\frac{u_x}{h} = \frac{1}{G}U\frac{\partial\tau_x}{\partial_y} + \frac{\tau_x\tau_o}{\tau_e\mu}f\left(\frac{\tau_e}{\tau_o}\right) \qquad [2a]$$

$$\frac{u_y}{h} = \frac{1}{G}U\frac{\partial\tau_y}{\partial_y} + \frac{\tau_y\tau_o}{\tau_e\mu}f\left(\frac{\tau_e}{\tau_o}\right) \qquad [2b]$$

where U is the rolling velocity. Also, note that y is the rolling direction.

Now using the notations

$$\bar{y} = \frac{y}{b} \text{ and } \bar{\tau} = \frac{\tau}{\tau_o}$$

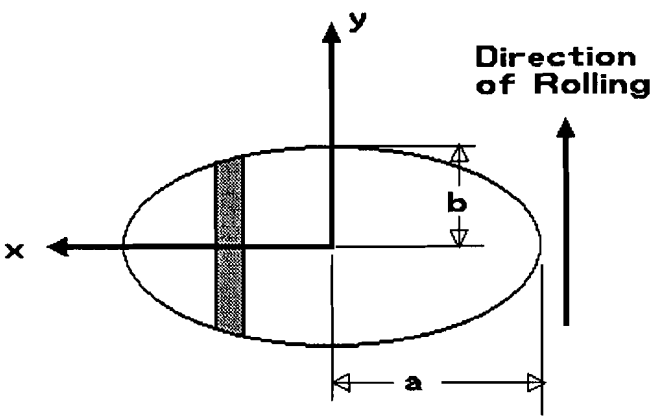

Fig. 1—Coordinates in the ball/race contact ellipse.

and by denoting the x and y direction by the subscript i with values of 1 and 2 corresponding to the two directions, Eq. [2] may be written as:

$$\frac{\partial\bar{\tau}_i}{\partial\bar{y}} = \bar{s}_i - \frac{1}{D}\frac{\bar{\tau}_i}{\tau_e}f(\bar{\tau}_e) \qquad [3]$$

where $\bar{s}_i = \frac{u_i}{h}\frac{Gb}{U\tau_o}$ is a dimensionless slip rate, and

$D = \frac{\mu U}{Gb}$ is the Deborah number.

The function $f\left(\frac{\tau_e}{\tau_o}\right)$, assumes a hyperbolic sine variation in the case of the Johnson and Tevaarwerk model (*6*), while an inverse hyperbolic tangent variation is substituted to implement the Bair and Winer model (*7*). The pertinent computational procedure is written such that both these options are easily available.

The ball/race contact ellipse is divided into several incremental strips, as shown schematically in Fig. 1. Equation [3] is now applied to calculate the local shear stresses on the strip, which are then integrated over the contact ellipse to compute total traction vector in the contact. Since, due to curvature effects, the local slip goes through zero at the points of pure rolling and then changes sign, it is essential to first solve the ball/race slip equation to determine the points of pure rolling. These points are then used to segment the contact zone. Thus, no slip discontinuity occurs in each segment of the contact zone. A Gaussian quadrature algorithm is then used to divide each segment into incremental strips of varying widths. Equation [3] is then integrated numerically over the incremental strip for a given slip distribution and prescribed rheological constants. A Runge-Kutta type integration algorithm is used to perform the integration in the range $-1 \leq \bar{y} \leq 1$. The initial condition is, of course, that the shear stress is zero at the inlet, $\bar{y} = -1$. Once the shear stress along the incremental strip is obtained, it may be integrated to compute traction force and moment on the incremental strip, which can be subsequently integrated to get the total traction force and moment.

TEST BEARING GEOMETRY AND OPERATING CONDITIONS

After implementing the traction models as described above, the dynamic performance of a typical high-speed gas turbine engine bearing is evaluated as a function of the rheological parameters. The geometry of the bearing is described in Table 1. In order to simulate a high-speed operation, a shaft speed of 20000 rpm is assumed, while a combined thrust of 4500 N and a stationary radial load of 2000 N is applied on the bearing. A MIL-L-7808 type oil at a bearing operating temperature of 350° K is assumed to lubricate the bearing. Although this operating temperature may be low for a high-speed bearing application, it is selected here quite arbitrarily to simulate a well-lubricated

TABLE 1—BEARING GEOMETRY AND MATERIAL PROPERTIES			
BEARING GEOMETRY			
Shaft Outside Diameter (mm)		100	
Shaft Inside Diameter (mm)		20	
Bearing Outer Diameter (mm)		180	
Housing Outer Diameter (mm)		205	
Number of Balls		18	
Ball Diameter (mm)		19.050	
Pitch Diameter (mm)		140.00	
Contact Angle (Deg)		25.00	
Outer Race Curvature Factor		0.52	
Inner Race Curvature Factor		0.54	
Outer Shrink Fit (microns)		10.00	
Inner Shrink Fit (microns)		50.00	
Cage Outer Diameter (mm)		146.292	
Cage Inner Diameter (mm)		130.073	
Cage Width (mm)		36.241	
Cage Outer Clearance (mm)		4.73583	
Cage Inner Clearance (mm)		1.46050	
Pocket Clearance (mm)		0.86360	
Cage Guide Land Width (mm)		8.00	
Guidance Type		Inner	
MATERIAL PROPERTY	BALLS	RACES	CAGE
Density (Kgm/M^3)	7750	7750	1000
Elastic Modulus (GPa)	200	200	200
Poisson's Ratio	0.25	0.25	0.25
Coeff of Ther Exp (1/°C)·10^5	1.17	1.17	1.17
Hardness (GPa)	7.845	7.845	0.008
Wear Coefficient · 10^6	5	5	500

condition with a relatively thick lubricant film. All lubricant properties in the ball/race contacts are assumed to be constant and equal to the effective average values computed at the prescribed operating conditions from the constitutive relations developed earlier (*2*). For the purpose of demonstrating the visco-elastic effects and the practical significance of the model, three sets of lubricant parameters are considered:

Case 1

In the first case, the lubricant viscosity, shear modulus and critical shear stress are derived directly from the MIL-L-7808 data presented earlier (*2*). At an average contact pressure of about 1.0 GPa and a temperature of 350° K, which represent the operating conditions in the bearing, effective values of the three lubricant parameters, viscosity, shear modulus and critical shear stress, are found to be 4.27 Pa.S, 27.5 MPa and 2.25 MPa respectively. Under the operating speed of 20000 rpm and the prescribed geometry of the bearing, the Deborah number varies in the range of 0.040 to 0.060. The variation is a result of difference in contact geometry at the outer and inner races and the ball-to-ball load variation due to the applied radial load. Clearly, the elastic effects in the lubricant will be negligible under such conditions and the lubricant behavior shall be essentially viscous.

Case 2

In order to introduce increased elastic effects, the shear modulus is reduced to 1.25 MPa in this case, while the other lubricant properties are held to be same as those in Case 1. The effective Deborah number is now in the range of 0.80 to 1.3. Moderate elastic effects may come into play under these conditions. Note that the deviation from properties used in Case 1, which represent actual behavior of the lubricant, is selected arbitrarily to demonstrate the significance of elastic effects. The increase in the Deborah number can also be brought about by changes in viscosity, operating temperature, etc.

Case 3

In order to significantly increase the Deborah number and the resulting elastic effects, the shear modulus in this case is reduced to 0.275 MPa. An equivalent effect may be realized by appropriate variations in the contact half width, rolling speed and lubricant viscosity. Both the shear modulus and viscosity will depend on operating pressure and temperature, while the contact half-width will be a function of bearing geometry, applied load and speed. Thus, it is a combination of the lubricant constitutive relation and operating conditions which determines the effective Deborah number and the resulting elastic effects. Similarly, the critical shear stress, which affects traction coefficients at high slip velocities, may depend on operating pressures and temperature. Again, to illustrate the effect of relatively low traction coefficient at high slip velocities, the critical shear stress in this case is reduced to 1.125 MPa.

It must be emphasized that neither the bearing geometry nor the operating conditions represent any specific application. The selection is really quite arbitrary and the variation in lubricant parameters is selected to demonstrate the significance of fundamental lubricant properties on the stability of the bearing elements and the overall dynamic behavior. All selected variations are strictly for illustrative purpose only.

To provide some estimate of the range of ball/race traction coefficients, Fig. 2 shows the calculated traction curves based on the Johnson and Tevaarwerk model (*6*). Results in the case of Bair and Winer (*7*) model are quite similar. The parametric evaluation in this paper is therefore restricted to the Johnson and Tevaarwerk model.

In terms of effects on the overall dynamics of the bearing elements, the traction curves shown in Fig. 2 for the three cases, provide a range of traction slopes at low slip velocities. Since this slope affects ball accelerations and the resulting

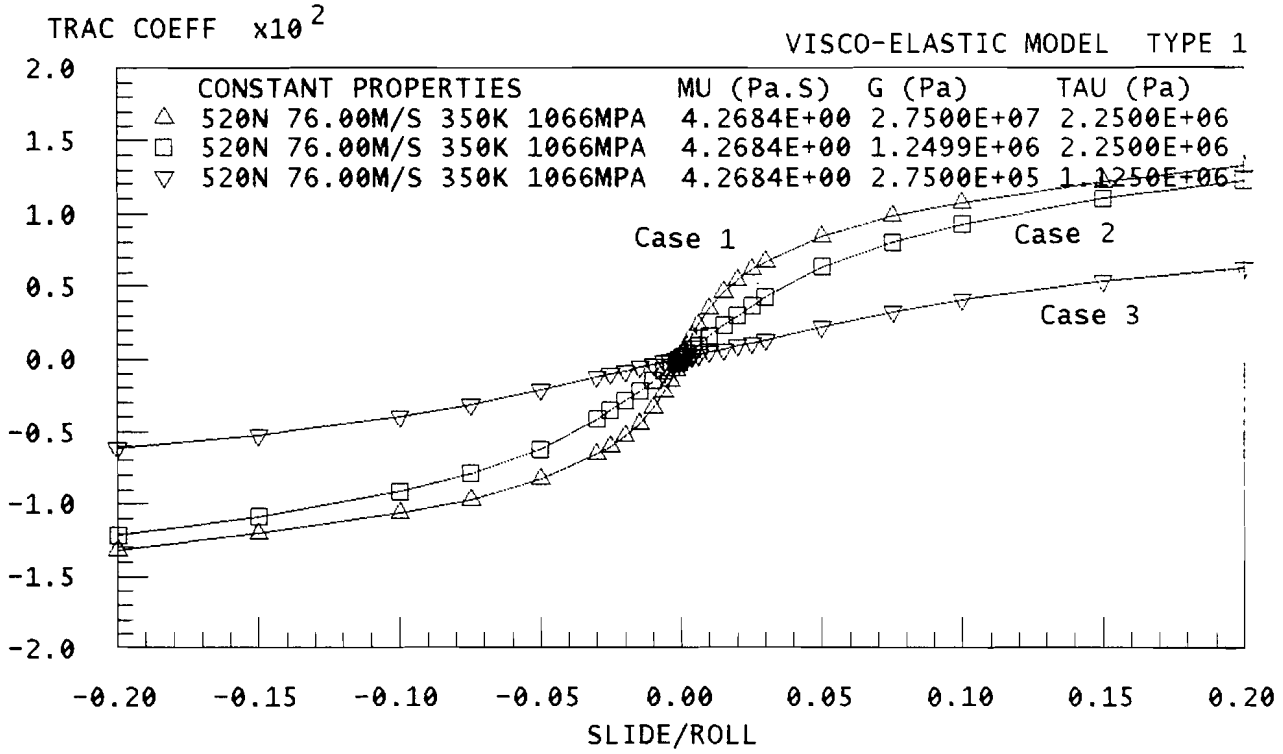

Fig. 2—Traction curves for the three sets of lubricant properties.

cage pocket forces, the selected data sets provide a rather interesting range of lubricant parameters to evaluate the significance of visco-elastic effects on overall bearing dynamics.

RESULTS

With the above modifications for the traction models, the bearing dynamics computer code ADORE is executed for the three cases of lubricant properties discussed above. The differential equations of motion of all the bearing elements are integrated over 2000 time steps, which resulted in bearing performance simulation over about 30, 27 and 18 shaft revolutions, respectively, for the three sets of lubricant parameters. In each case, the solutions generated are found to be adequate to evaluate the expected steady-state behavior of the bearing.

As might be expected, a reduced traction slope within the three data sets results in an increase in ball/race slip velocities. Figure 3 plots the variation in maximum ball/race slip velocity in the contact, for Cases 1, 2 and 3. Although there is little change in the results between Cases 1 and 2, a noticeable increase in the slip velocity is seen in Case 3, which corresponds to the lowest traction slope in Fig. 2. The maximum sliding velocity shown this figure is actually the magnitude to the largest slip vector, and it contains the slip contributions from sliding in the direction of rolling, relative ball spin about an axis normal to the plane of contact, and lateral sliding due to gyroscopic rotation of the ball. The high slip value of 10 m/s, seen in Case 3, results in a slide-to-roll ratio of 0.13 with the rolling velocity of about 76 m/s when the bearing operates at 20000 rpm. Clearly, with such operating conditions there will be some points in the contact ellipse where the critical shear stress parameter has a notable effect on traction.

The lubrication parameters have the most significant effect on the cage motion. The increasing ball slip with reducing traction slope results in increasing cage interactions. Figures 4, 5, and 6 show the cage forces for Cases 1, 2 and 3 respectively. The figures show the guide land force, typical cage pocket forces (Pocket #1), and an overall cage interaction which is defined in terms of a time-averaged wear rate, which really represents a load-velocity integral:

$$W(T) = \frac{1}{T}\int_0^T \frac{K}{H} P(t)V(t)dt$$

where W is the time-averaged wear rate over time T, when the contact load, sliding velocity, hardness of the material and an Archard-type wear coefficient are respectively denoted by P, V, H, and K.

A close comparison of these figures reveals several interesting findings. First, note the large increase in the frequency of ball/cage collisions and the drastic increase in pocket forces in Fig. 6, which represents Case 3 with the lowest traction slope. There is no significant difference in pocket forces for Cases 1 and 2, shown respectively in Figs. 4 and 5. The increase in pocket interactions results in a corresponding increase in the guide land forces at the cage/race interface. Note that in all cases, after a few transients, the cage tends to come in steady contact with the race. The contact force in Case 3 is almost double of what is seen in Cases 1 and 2. Finally, a comparison of the time-averaged wear rate reveals that while the cage interactions stabilize to essentially similar values in Cases 1 and 2, the wear rate

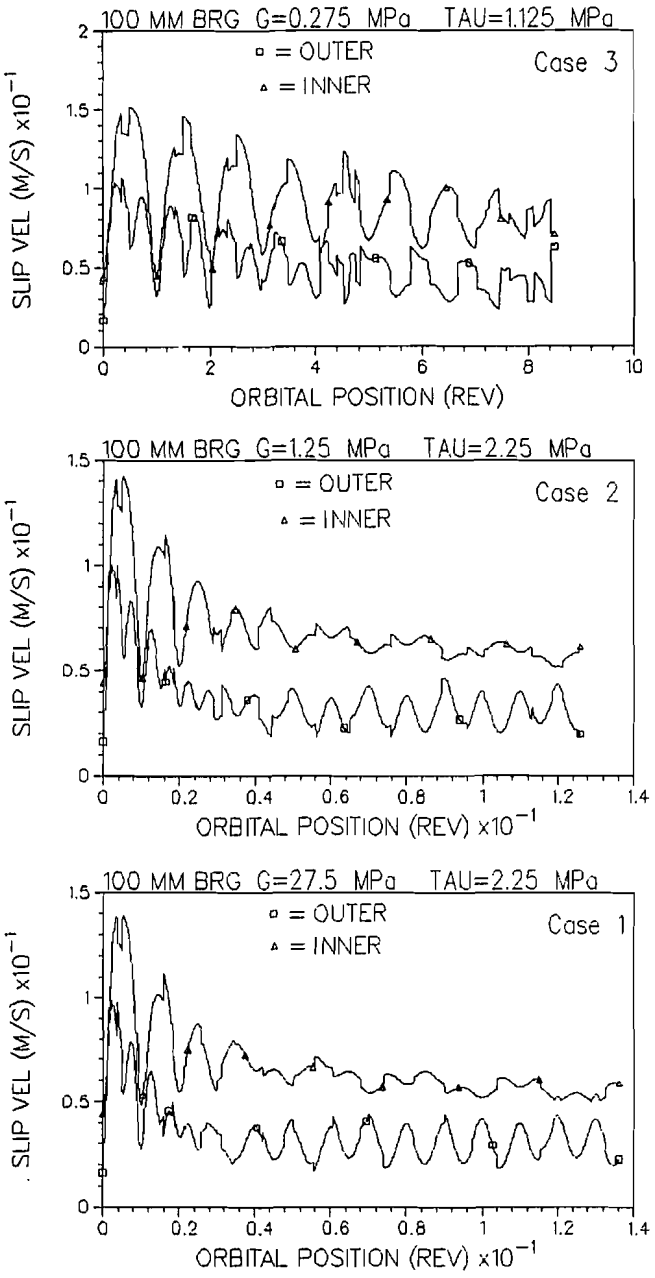

Fig. 3—The effect of lubricant properties on ball/race slip velocities.

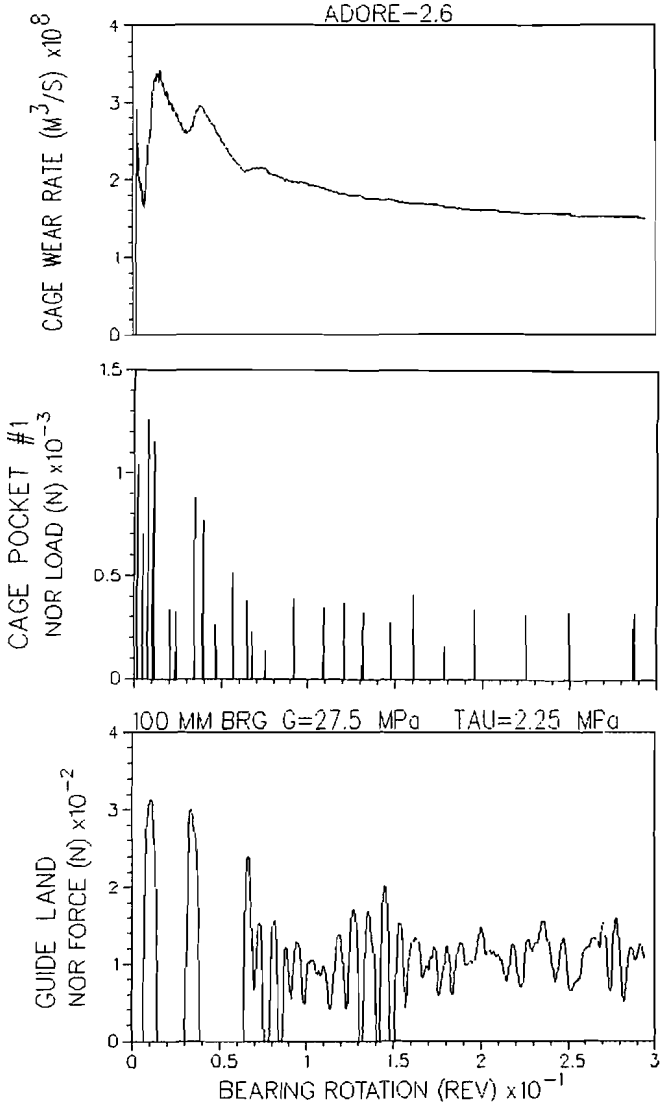

Fig. 4—Cage interactions with lubricant properties of Case 1.

is steadily increasing to significant larger values in Case 3. Such an increase implies that either the contact forces or the sliding velocities, or perhaps both, are increasing with time. It therefore represents a kind of instability in the overall cage interactions.

The effect on cage motion and stability is further seen by examining the mass center whirl orbits, in a plane normal to the bearing axis, for the three data sets, as shown respectively in Figs. 7, 8 and 9. In each case, the cage starts off from a small negative displacement in the Z direction, which is really a prescribed initial condition for the integration of the differential equations of cage motion. A positive rotation about the X axis, according to the right hand screw rule, is along the direction of bearing rotation. In Cases 1 and 2, the cage assumes a fairly well-defined whirl with a speed ratio, defined as whirl divided by the shaft velocity, of 0.30. In Case 3, however, whirl is quite erratic. In fact, as seen in Fig. 9, a very slow negative whirl, with a whirl ratio = -0.066, develops after the initial transients.

The above results clearly demonstrate the significance of lubricant properties of the overall bearing performance, particularly the cage motion. The intuitive assumption that a reduction in traction leads to improved bearing performance and stability may not always be true. Perhaps it is the traction slope which controls the bearing performance, and it may be essential for this slope to be within a range for stable performance. In terms of the visco-elastic behavior, note that in Case 3, where the shear modulus is lowest, the Deborah number is the highest of the three cases. This implies that the elastic behavior is relatively more prominent in Case 3. Thus, the motion of the cage becomes unstable as the elastic effects in the lubricant become more pronounced. Such a finding hints at a relation between cage stability and the effective Deborah number. Such a relation, if it exists, has a substantial practical significance, both for characterizing dynamic bearing behavior, and for developing lubricants for critical operating environments. A much more extensive parametric evaluation than that considered here is, of course, required before such a relationship can

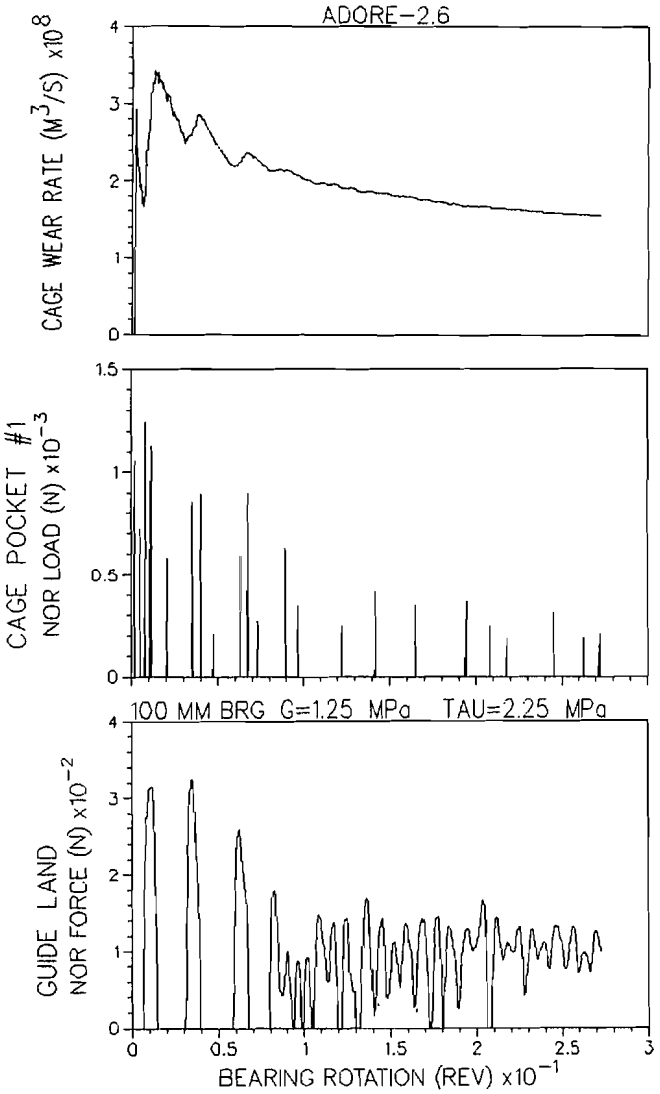

Fig. 5—Cage interactions with lubricant properties of Case 2.

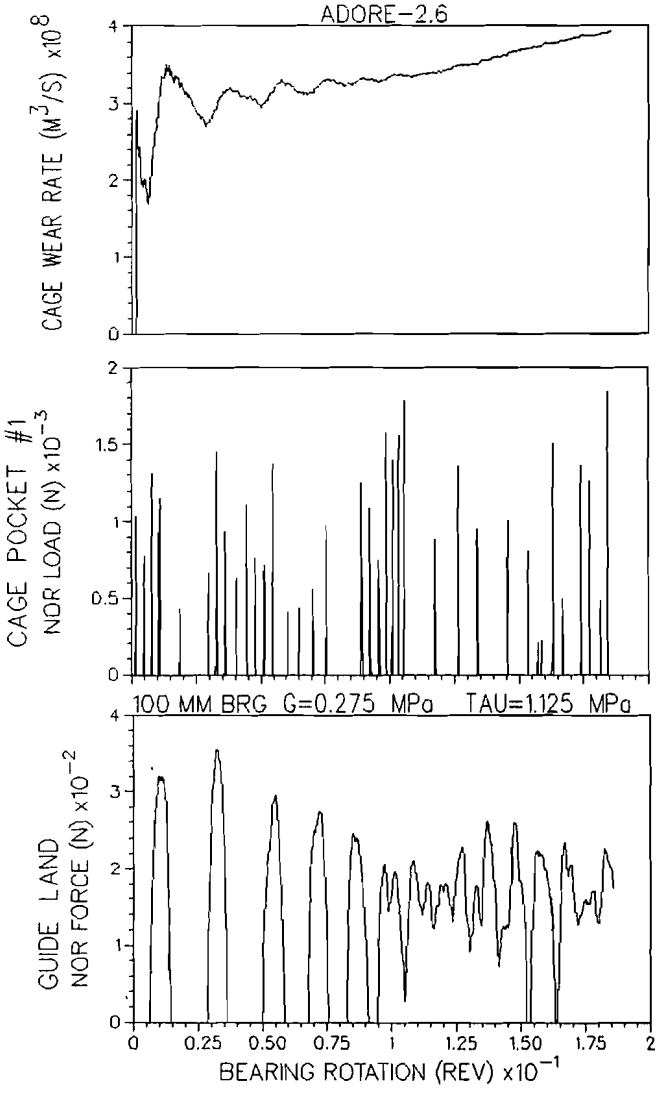

Fig. 6—Cage interactions with lubricant properties of Case 3.

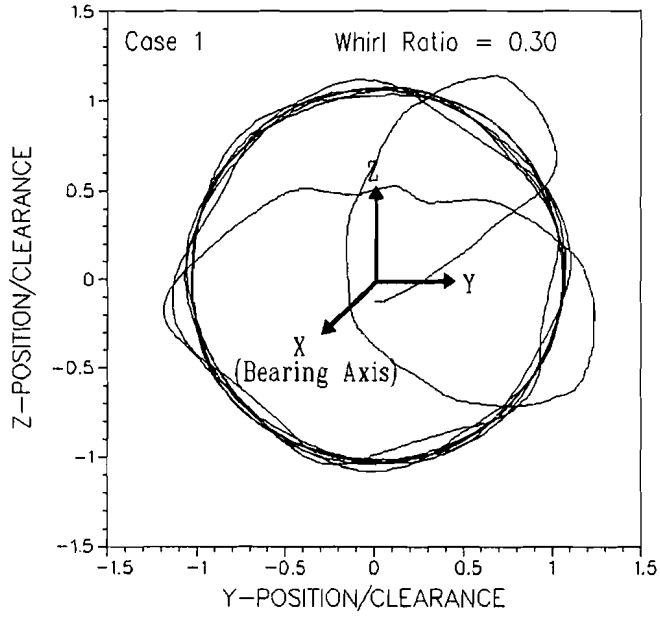

Fig. 7—Cage mass center whirl with lubricant properties of Case 1.

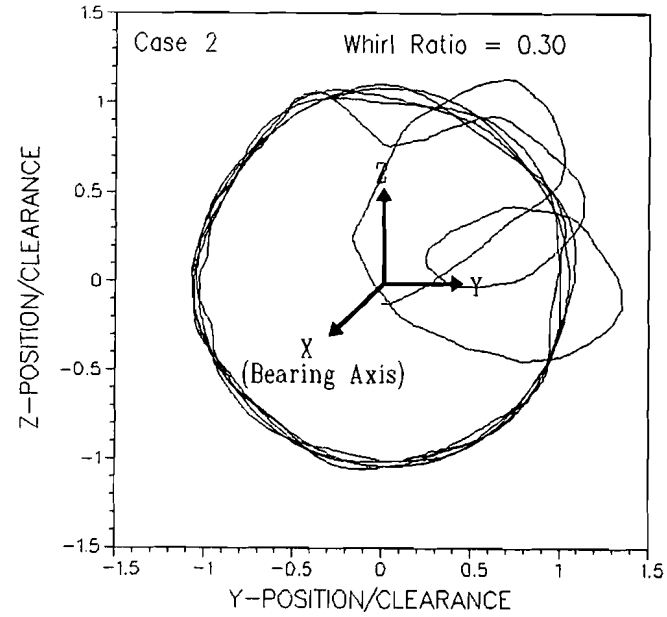

Fig. 8—Cage mass center whirl with lubricant properties of Case 2.

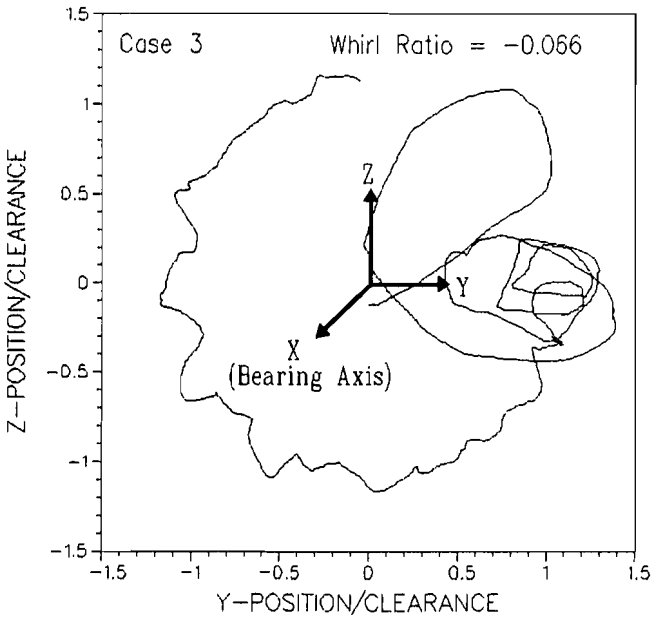

Fig. 9—Cage mass center whirl with lubricant properties of Case 3.

be truly established. Also, as is true with any modeling effort, experimental validation of the computer predictions is essential before such a correlation can be used for practical design.

CONCLUSIONS

The analytical bearing performance simulations, obtained by integrating the differential equations of motion of the bearing elements under prescribed bearing geometry, operating conditions, and lubricant properties demonstrate a substantial practical significance of the Johnson and Tevaarwerk (*6*) model. As the shear modulus is reduced, the reducing traction slope at low slip velocities results in increasing ball slip and cage interactions. At the low values of the critical shear stress and shear modulus, when the elastic effects are most prominent, as indicated by the high Deborah number, the cage interactions become excessive and the motion becomes relatively unstable. Such a finding suggests that stability of the bearing elements could be possibly related to the fundamental properties of the lubricant. However, parametric evaluation of bearing performance, over a much wider range of parameters than that considered in this investigation, is essential before such a conclusion can be adequately supported.

ACKNOWLEDGMENTS

This work was sponsored by the Aero Propulsion and Power Laboratory at Wright-Patterson Air Force Base, contract number F33615-86-C-2696, under the Defense Small Business Innovation Research Program with Mr. Nelson H. Forster, WRDC/POSL, as the project engineer. Computational support was provided by the ASD Computer Center at Wright-Patterson Air Force Base.

REFERENCES

(*1*) Gupta, P. K., Cheng, H. S., Zhu, D., Forster, N. H. and Schrand, J. B., "Visco-Elastic Effects in MIL-L-7808-Type Lubricant, Part I: Analytical Formulation," *Trib. Trans.*, **35**, 2, pp ???–??? (1992).

(*2*) Forster, N. H., Schrand, J. B. and Gupta, P. K., "Visco-Elastic Effects in MIL-L-7808 Type Lubricant, Part II: Experimental Data Correlations," *Trib. Trans.*, **35**, pp ???–??? (1992).

(*3*) Kannel, J. W., Bupara, S. S. and Pentlicki, C. J., "Investigation of Cage and Bearing Stability in Despun Antenna Bearings Due to Changes in Lubricant Properties," U.S. Air Force Report **AFML-TR-75-38**, Wright-Patterson Air Force Base, Ohio (1976).

(*4*) Gupta, P. K., "Frictional Instabilities in Ball Bearings," *Trib. Trans.*, **31**, 2, pp 258–268 (1988).

(*5*) Rivera, M. P., "Bearing-Cage Frictional Instability—A Mechanical Model," *Trib. Trans.*, **34**, pp 117–121 (1991).

(*6*) Johnson, K. L. and Tevaarwerk, J. L., "Shear Behavior of EHD Oil Films," *Proc. Royal Soc. London*, **A356**, p 215 (1977).

(*7*) Bair, S. and Winer, W. O., "A Rheological Model of EHD Contacts based on Primary Laboratory Data," *ASME Jour. of Lubr. Tech.*, **101**, 3, p 258 (1979).

(*8*) Gupta, P. K., Advanced Dynamics of Rolling Elements, Springer-Verlag, Berlin (1984).

(*9*) Hamrock, B. J. and Dowson, D., "Isothermal Elastohydrodynamic Lubrication of Point Contacts, Part III–Fully Flooded Results, *ASME Jour. of Lubr. Tech.*, **99**, 2, pp 264–276 (1977).

(*10*) Wilson, W. R. D. and Sheu, S., "Effect of Inlet Shear Heating Due to Sliding on Elastohydrodynamic Film Thickness," *ASME Jour. of Lubr. Tech.*, **105**, pp 187–188 (1983).

(*11*) McCool, J. I., "Evaluating the Tevaarwerk-Johnson Elastic/Plastic Traction Model in the Presence of Lateral Sliding and Spin," *Trib. Trans.*, **33**, pp 122–130 (1990).